

## 基于转录组学测序与生物信息学筛选低氧诱导小鼠肾脏炎症反应的关键基因并验证

许鑫桐, 龙启福, 胡英, 贾茹涵, 马如雪, 永胜  
(青海大学医学院基础医学部, 西宁 810016)

**摘要** **目的** 利用转录组学测序与生物信息学挖掘低氧诱导小鼠肾脏炎症反应的关键基因并验证。**方法** 于海拔4 200 m和海拔400 m分别饲养C57/BL6小鼠, 构建高原低氧组和平原常氧组小鼠模型, 30 d后无菌取出小鼠肾脏组织, HE染色分析肾脏病理学变化, 并测定低氧暴露下小鼠血气分析和肾脏指数改变。然后对高原低氧组和平原常氧组小鼠肾脏组织进行转录组学测序分析, 并利用生物信息学技术筛选关键基因, 通过实时定量逆转录PCR (RT-qPCR) 和Western blotting对关键基因进行验证。**结果** HE染色结果显示与平原常氧组比较, 高原低氧组小鼠肾小球萎缩, 低氧暴露下小鼠血气分析和肾脏指数均下降。转录组学测序分析结果显示, 高原低氧组中共有3 007个差异表达基因, 其中123个是与炎症相关的差异表达基因 (IR-DEGs)。对IR-DEGs进行GO和KEGG富集分析结果显示, 在细胞因子-细胞因子受体相互作用、趋化因子等炎症相关信号通路显著富集。对IR-DEGs构建蛋白质-蛋白质相互作用 (PPI) 网络结果显示, 共鉴定出STAT3、TLR7、CD68、NFKBIA、LEP、APOE 6个Hub基因。RT-qPCR检测结果显示, 6个Hub基因的mRNA表达均上调, 与转录组测序结果一致。Western blotting检测结果显示, CD68、NFKBIA、LEP、TLR7和APOE蛋白表达上调, STAT3表达下调。**结论** STAT3、CD68、NFKBIA、LEP、TLR7和APOE是低氧诱导炎症反应的关键基因。低氧环境通过上调机体TLR7、CD68、STAT3、LEP、APOE的表达, 诱导小鼠肾脏组织发生炎症反应。

**关键词** 高原低氧; 肾脏; 炎症反应; 转录组学测序; 生物信息学

中图分类号 R34 文献标志码 A 文章编号 0258-4646(2024)12-1071-09

网络出版地址 <https://link.cnki.net/urlid/21.1227.R.20241206.1532.028>

DOI: 10.12007/j.issn.0258-4646.2024.12.003

### Screening and validation of key genes for hypoxia-induced renal inflammatory reaction in mice by transcriptome sequencing and bioinformatics

XU Xintong, LONG Qifu, HU Ying, JIA Ruhan, MA Ruxue, YONG Sheng  
(Department of Basic Medicine, College of Medicine, Qinghai University, Xining 810016, China)

**Abstract** **Objective** To screen and validate the key genes involved in hypoxia-induced inflammatory reactions in mice using transcriptome sequencing and bioinformatics. **Methods** C57/BL6 mice were bred at altitudes of 4 200 m and 400 m, and mouse models were constructed for the plateau hypoxia (HKT) group and the plain normoxia (PKC) group. Kidney tissues were aseptically removed after 30 days, renal pathological changes were analyzed by HE staining, blood gas analysis and renal index changes were measured in the mice under hypoxia. The kidney tissues of mice in the HKT and PKC groups were analyzed using transcriptome sequencing, key genes were screened using bioinformatics technology, and these genes were verified using real-time quantitative reverse transcription PCR (RT-qPCR) and Western blotting. **Results** HE staining showed glomerular atrophy in mice in the HKT group compared with the PKC group, and a decrease in blood gas analysis and renal index occurred in mice exposed to hypoxia. Transcriptome sequencing analysis revealed 3 007 differentially expressed genes (DEGs) in the HKT group, of which 123 were inflammation-related DEGs (IR-DEGs). GO and KEGG enrichment analyses of IR-DEGs showed significant enrichment in inflammation-related signaling pathways, such as cytokine-cytokine receptor interactions and chemokines. The results of the protein-protein interaction (PPI) network construction of IR-DEGs showed that six hub genes, STAT3, TLR7, CD68, NFKBIA, LEP, and APOE, were identified, and the mRNA expression of these six genes was upregulated according to RT-qPCR results, which was in agreement with the results of transcriptome sequencing. Western blotting showed that CD68, NFKBIA, LEP, TLR7, and APOE expression was upregulated while STAT3 expression was downregulated. **Conclusion** STAT3, CD68, NFKBIA, LEP, TLR7, and APOE are the key genes involved in hypoxia-induced inflammatory reactions. A hypoxic environment induced inflammatory reactions in mouse kidney tissues by upregulating the expression of TLR7, CD68, STAT3, LEP, and APOE.

**Keywords** plateau hypoxia; kidney; inflammatory reaction; transcriptome sequencing; bioinformatics

基金项目: 国家自然科学基金 (82060295)

作者简介: 许鑫桐 (1999-), 男, 硕士研究生。

通信作者: 永胜, E-mail: yongsheng@qhu.edu.cn

收稿日期: 2023-12-25

网络出版时间: 2024-12-09 12:16:47

高海拔环境具有低压、低氧的特点,能使人体动脉血氧分压(partial pressure of oxygen, PaO<sub>2</sub>)和血氧饱和度(saturation oxygen, SaO<sub>2</sub>)降低;当低氧应激超过机体的适应能力时,会导致组织缺氧而影响机体正常的生理功能,轻者表现为高原反应,重者则会诱发高原肺水肿、高原脑水肿等急性反应<sup>[1-2]</sup>。肾脏由于具有复杂的血管结构、溶质重吸收功能及抗氧化防御能力较弱等特征,更容易缺氧<sup>[3]</sup>。肾耗氧量与钠转运关系密切,肾小管中的钠离子重吸收消耗约80%总氧,而其余20%总氧消耗与肾脏的基础代谢相关<sup>[4]</sup>。此外,低氧环境可以刺激高原居民不同组织和细胞中促炎和抗炎细胞因子的表达<sup>[5]</sup>。

缺氧诱导因子-1 $\alpha$ (hypoxia-inducible factor-1 $\alpha$ , HIF-1 $\alpha$ )表达和炎症反应的发生关系密切。研究<sup>[6]</sup>发现,小鼠体内缺乏HIF-1 $\alpha$ 的巨噬细胞不能对炎症刺激产生炎症反应。在机体处于低氧状态时,HIF-1 $\alpha$ 在细胞中不断累积,激活氧化应激<sup>[7]</sup>,此过程对慢性肾脏病(chronic kidney disease, CKD)的发生发展具有重要作用。氧化应激激活肾脏细胞内的炎性细胞因子,损伤肾小球内皮细胞,引起内皮功能紊乱,促进CKD发病<sup>[8-9]</sup>。此外,活性氧(reactive oxygen species, ROS)可以激活相关转录因子,启动肾间质纤维化过程<sup>[10]</sup>,从而参与CKD的进展。研究发现,相比于健康人群,CKD未透析患者血清中白细胞介素(interleukin, IL)-16、C反应蛋白(C-reactive protein, CRP)水平显著升高<sup>[11]</sup>。CKD患者机体长期处于微炎症状态,表现出微炎症标志物增加,并随着CKD加重而增长<sup>[12]</sup>。炎症反应通过激活中性粒细胞的NADPH氧化酶,促进ROS大量产生,而体内大量ROS激活核转录因子促进炎症介质释放<sup>[13]</sup>,炎症介质也可以进一步促进ROS的产生,加剧CKD的发生和发展<sup>[14-15]</sup>。然而,低氧环境引起肾脏组织发生炎症反应的关键基因及相关机制尚未明确。

本研究选取高原低氧条件下小鼠作为研究对象,对其进行转录组学测序分析,利用生物信息学筛选关键的差异表达基因(differential expressed genes, DEGs)并验证,旨在为明确高原低氧环境下小鼠肾脏组织炎症反应的分子机制提供依据。

## 1 材料与方法

### 1.1 实验动物及低氧模型构建

10只6~8周龄C57BL/6雄性小鼠,体重(18±2)g,购自西安交通大学医学部实验动物中心,动物许可证号为SYXK(陕)2020-005。随机将小鼠分为平原常氧组(PKC组)和高原低氧组(HKT组),每组5只。PKC组饲养于海拔400 m的西安交通大学实验动物中心,HKT组饲养于海拔4 200 m的青海省玛多县人民医院实验动物房,期间保证饲养条件一致。30 d后无菌采集小鼠肾脏组织,一部分组织于4%多聚甲醛中固定保存,另一部分置于液氮中速冻保存。本研究获得青海大学医学伦理委员会批准。

### 1.2 肾脏指数测定

测量小鼠空腹时体重,随后将小鼠双侧肾脏组织取出,滤纸吸干肾脏表面血水并使用电子天平称量,计算肾脏指数:肾脏指数=双侧肾重量(g)/体重(g)×100%。

### 1.3 动脉血气分析

麻醉小鼠后打开腹腔,用注射器无菌抽取小鼠右侧腹主动脉血。PT1000湿式血气分析仪及配套试剂(武汉明德生物科技股份有限公司)测量小鼠动脉SaO<sub>2</sub>及PaO<sub>2</sub>。

### 1.4 HE染色检测肾脏组织病理学改变

取浸于4%多聚甲醛固定48 h的小鼠肾脏组织,石蜡包埋,切片机切成5~6  $\mu$ m薄片,脱蜡、苏木精和伊红染色。光学显微镜下观察肾脏组织切片。

### 1.5 高通量转录组学测序

使用TRIzol试剂盒提取肾脏组织总RNA,并评估RNA质量,测量其浓度、纯度及完整性。随后进行cDNA文库构建,使用PCR技术扩增文库,为降低杂质对构建文库的影响对文库进行纯化。测序由北京诺禾致源有限公司运用Illumina测序平台完成。

### 1.6 DEGs分析

通过R语言包DESeq2对基因表达矩阵进行分析,将调整 $P < 0.05$ 且 $|\log_2FC| \geq 0$ 作为筛选DEGs的表达阈值。使用R语言包ClusterProfiler对DEGs进行基因本体(gene ontology, GO; <http://www.geneontology.org/>)、京都基因和基因组数据库(Kyoto Encyclopedia of Genes and Genomes, KEGG; <http://www.genome.jp/kegg/pathway.html>)富集分析。

### 1.7 炎症相关的差异表达基因(inflammation related-differential expressed genes, IR-DEGs)筛选及功能分析

从Ensembl在线数据库(<https://asia.ensembl.org/>)

index.html) 获得760个炎症反应相关基因 (inflammation related genes, IRGs)。DEGs与IRGs交集获得IR-DEGs。对IR-DEGs进行GO和KEGG富集分析。

### 1.8 IR-DEGs的蛋白质-蛋白质相互作用 (protein-protein interaction, PPI) 网络构建与Hub基因筛选

使用STRING数据库 (<http://string-db.org/>) 和Cytoscape软件3.9.1 (<http://cytoscape.org/>) 分析IR-DEGs的相互作用构建PPI网络<sup>[16]</sup>。利用CytoHubba插件根据最大集团中心性 (maximum clique centrality, MCC)、度和边缘渗透分量 (edge percolated component, EPC) 算法进行筛选, 利用3种不同计算方法分别筛选出

排名前10位的基因, 然后取交集获得排名前6位的基因为Hub基因。

### 1.9 实时定量逆转录PCR (real-time quantitative reverse transcription PCR, RT-qPCR) 检测

使用PrimeScript™ RT反转录试剂盒合成cDNA, 并采用TB Green嵌合荧光法进行RT-qPCR。 $\beta$ -actin作为内参, Livak法计算基因mRNA相对表达量, 引物序列见表1。20  $\mu$ L的反应体系中包括TB Green® Premix Ex Taq™ II 10  $\mu$ L, dH<sub>2</sub>O 6.4  $\mu$ L, cDNA 2  $\mu$ L, 正向和反向引物各0.8  $\mu$ L。

### 1.10 Western blotting检测

表1 基因引物序列

Tab.1 Gene primer sequences

Gene	Primer sequence	Length (bp)
$\beta$ -actin	Forward, 5'-CATCCGTAAGACCTCTATGCCAAC-3'	25
	Reverse, 5'-ATGGAGCCACCGATCCACA-3'	19
NFKBIA	Forward, 5'-CTGAAAGCTGGCTGTGATCCTGAG-3'	24
	Reverse, 5'-CTGCGTCAAGACTGCTACACTGG-3'	23
STAT3	Forward, 5'-AATCTCAACTTCAGACCCGCCAAC-3'	24
	Reverse, 5'-GCTCCACGATCCTCTCCTCCAG-3'	22
TLR7	Forward, 5'-AAAGCCCTTTACCTGGATGGAAAC-3'	24
	Rreverse, 5'-TCGTGATGGAGAAGATGTTGTTAGC-3'	25
CD68	Forward, 5'-CCTCTTGCTGCCTCTCATATTGG-3'	24
	Reverse, 5'-GGCTGGTAGGTTGATTGTCGTCTG-3'	25
LEP	Forward, 5'-TCCTGTGGCTTTGCTCTATCTG-3'	23
	Reverse, 5'-CCTGGTGACAATGCTCTTGATGAG-3'	24
APOE	Forward, 5'-CGAGGGCGCTGGAGGAAG-3'	23
	Reverse, 5'-TGCAAGTGCATCATCGTTGTTCC-3'	22

无菌取出小鼠肾脏组织, 研磨、裂解、超声处理后取上清液, BCA试剂盒测定蛋白浓度。30  $\mu$ g/孔上样, 随后电泳、转膜, 5%脱脂牛奶进行封闭、洗膜, 加入稀释后一抗4  $^{\circ}$ C孵育过夜, 取出后加入相关二抗室温孵育1 h。ECL化学发光液显色, 使用凝胶成像系统 (法国VILBER BIO IMAGING公司) 观察并检测蛋白质条带信号, 采用ImageJ软件分析蛋白表达量。

### 1.11 统计学分析

采用SPSS 27.0软件进行数据分析, 计量资料采用 $\bar{x} \pm s$ 表示。2组比较采用独立样本t检验。 $P < 0.05$ 为差异有统计学意义。

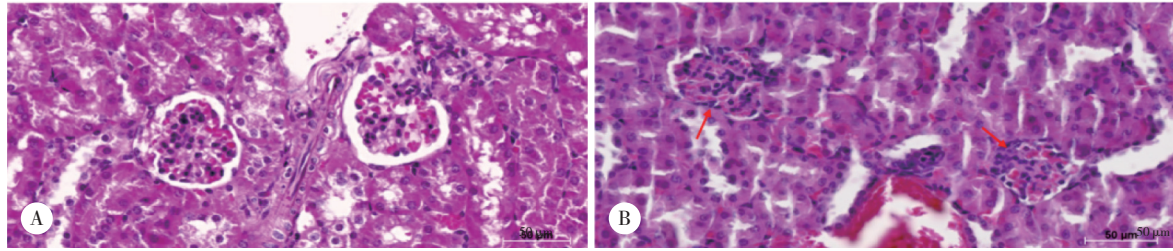
## 2 结果

### 2.1 2组小鼠HE染色、肾脏指数和血气分析结果

结果显示, 与PKC组比较, HKT组小鼠肾小球明显萎缩, 提示高原低氧环境下小鼠肾脏组织发生病理改变。见图1。与PKC组比较, HKT组小鼠体重、肾重量和肾脏指数均显著下降 ( $P < 0.001$ )。动脉血气分析结果显示, 与PKC组比较, HKT组小鼠PaO<sub>2</sub>、SaO<sub>2</sub>均显著下降 ( $P < 0.001$ ), 表明低氧动物模型构建成功。见表2。

### 2.2 测序数据质量评估

对转录组测序结果进行质量评估发现, PKC组和HKT组中过滤后的读长分别占原始数据的95.19%、90.45% (图2A), 而且每个样本的Q20和Q30分别>98.1%和>94.64% (图2B), 说明样本的测序数据过滤情况良好, 测序准确度较高, 可用于后续分析。



A, PKC group; B, HKT group.

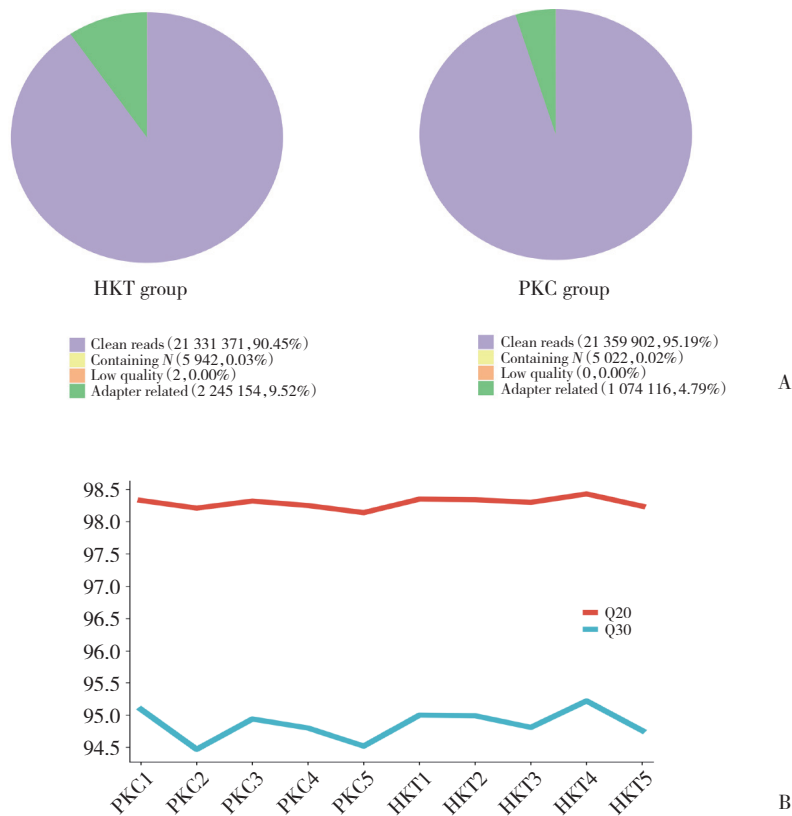
图1 2组小鼠肾脏组织HE染色结果

Fig.1 HE staining of kidney tissues in two groups of mice

表2 各组肾脏指数和血气分析结果比较

Tab.2 Comparison of renal index and blood gas analysis between two groups

Group	Kidney weight (g)	Body weight (g)	Kidney index (%)	PaO <sub>2</sub> (mmHg)	SaO <sub>2</sub> (%)
PKC	0.064 ± 0.003	22.602 ± 0.990	0.283 ± 0.008	94.115 ± 7.715	95.612 ± 1.136
HKT	0.045 ± 0.002	19.283 ± 0.538	0.223 ± 0.008	63.563 ± 7.187	81.565 ± 2.792
<i>t</i>	10.250	5.904	10.390	5.795	9.187
<i>P</i>	<0.000 1	<0.001	<0.000 1	<0.001	<0.000 1



A, percentage of clean reads in the HKT group versus the PKC group; B, percentage of Q20 and Q30 for each sample.

图2 测序数据质量评估

Fig.2 Sequencing data quality assessment

2.3 DEGs筛选及富集分析

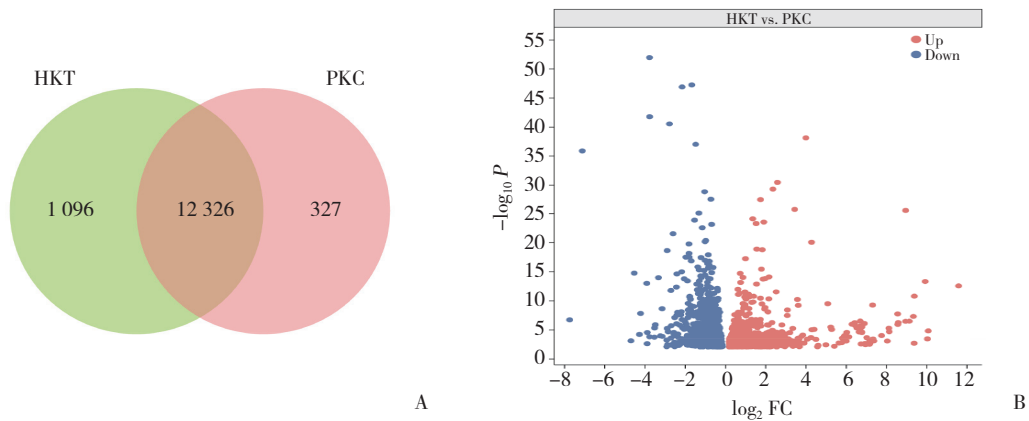
肾脏组织测序结果显示, HKT组有1 096个特

有表达基因, PKC组有327个特有表达基因, PKC组和HKT组有12 326个共表达基因(图3A)。共鉴定

筛选出3 007个DEGs, 其中1 349个基因表达上调, 1 658个基因表达下调(图3B)。KEGG通路富集分析表明, DEGs主要富集到IL-17、PPAR、mTOR、AMPK、凝血与补体、B细胞受体等炎症反应相关通路(图

4A)。GO富集分析显示, DEGs主要分布在生物过程的核糖磷酸代谢、细胞组分的线粒体蛋白复合体、分子功能的核糖体结构等(图4B)。

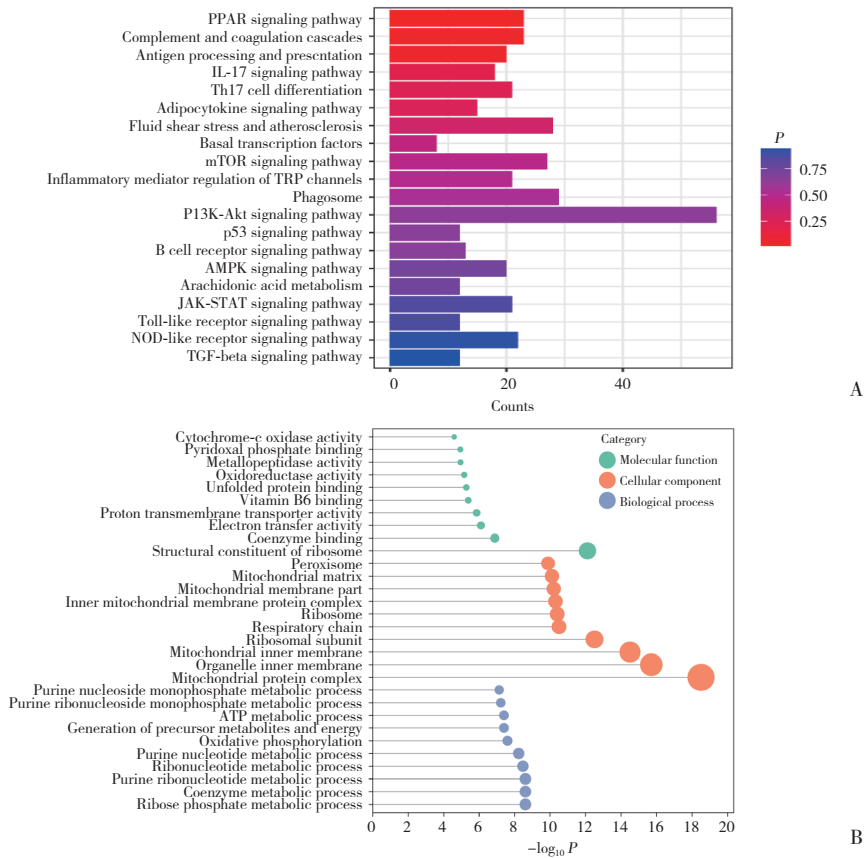
### 2.4 IR-DEGs筛选和功能富集分析



A, Wayne diagram; B, expression profile analysis of DEGs.

图3 DEGs的筛选

Fig.3 Screening of DEGs



A, KEGG enrichment analysis of DEGs; B, GO enrichment analysis of DEGs.

图4 DEGs的功能富集分析

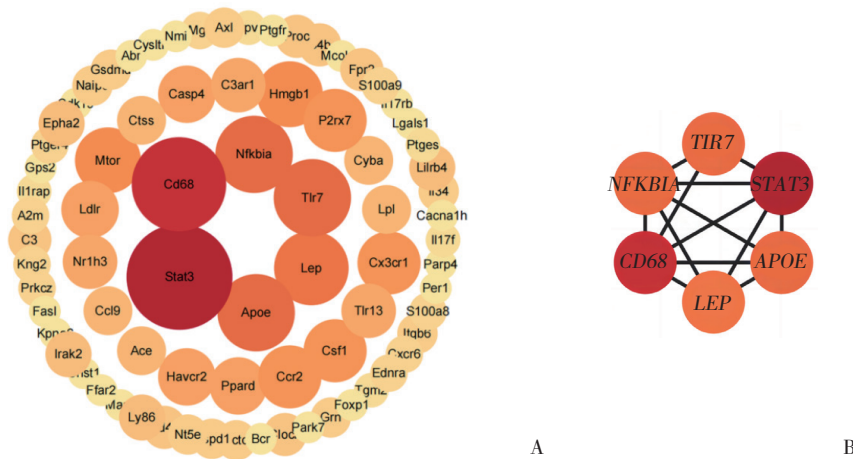
Fig.4 Functional enrichment analysis of DEGs



### 2.5 Hub基因筛选

利用String数据库建立IR-DEGs的PPI网络。网络节点数为123,边数为264(图7A)。通过CytoHubba插件分析,利用3种不同计算方法分别筛选出排名前10位的基因,交集后获得信号转导及转录激活蛋白3

(signal transducer and activator of transcription 3, *STAT3*)、瘦素 (leptin, *LEP*)、核因子- $\kappa$ B 抑制因子 $\alpha$  (nuclear factor kappa-B inhibitory alpha, *NFKBIA*)、Toll样受体7 (Toll-like receptors 7, *TLR7*)、载脂蛋白E (apolipoprotein E, *APOE*)、*CD68* 6个Hub基因(图7B)。



A, PPI network map; B, hub genes.

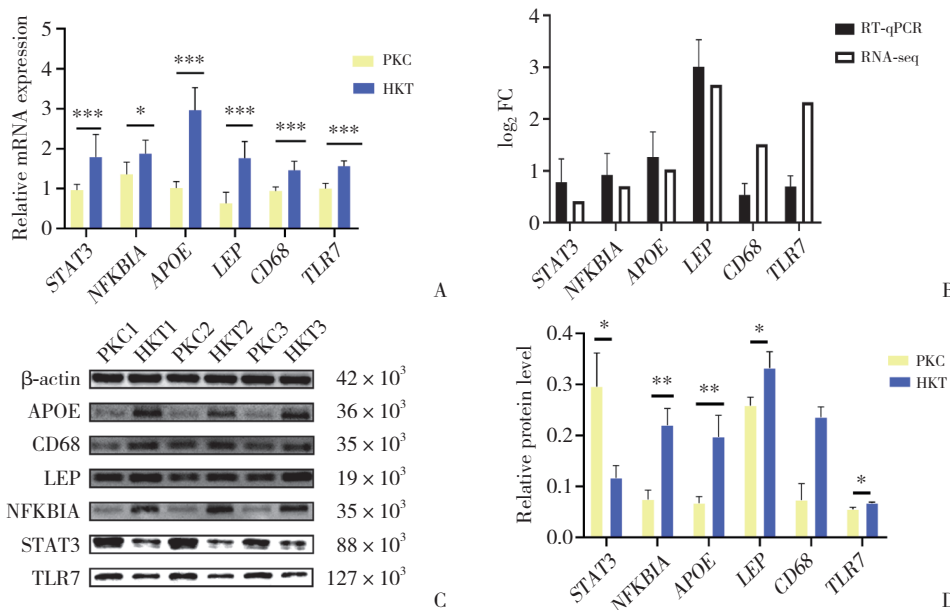
图7 IR-DEGs的PPI网络和Hub基因筛选

Fig.7 PPI network and hub gene screening in IR-DEGs

### 2.6 Hub基因验证

RT-qPCR检测结果显示,与PKC组比较,HKT组 *STAT3*、*NFKBIA*、*CD68*、*TLR7*、*LEP*、*APOE* mRNA表达均上调(均  $P < 0.05$ ,图8A),并且基因表达趋势与

转录组测序结果一致(图8B)。Western blotting检测结果显示,与PKC组比较,HKT组 *NFKBIA*、*LEP*、*TLR7*、*CD68*和 *APOE* 蛋白表达显著上调,而 *STAT3* 蛋白表达显著下调(均  $P < 0.05$ ,图8C、8D)。



A, RT-qPCR results of hub genes; B, results of hub genes compared with transcriptome; C, protein expression of six hub genes; D, quantitative analysis of protein expression of six hub genes, \*  $P < 0.05$ , \*\*  $P < 0.01$ , \*\*\*  $P < 0.001$ .

图8 Hub基因验证

Fig.8 Hub gene validation

### 3 讨论

本研究构建平原常氧和高原低氧小鼠模型。血气分析结果显示小鼠动脉血中PaO<sub>2</sub>、SaO<sub>2</sub>降低,提示成功建立了高原低氧小鼠模型。HE染色结果发现低氧暴露下小鼠肾小球发生明显萎缩,且小鼠体重、肾重量、肾脏指数均下降。表明高原低氧环境诱导肾脏产生了显著的病理改变。

进一步分析2组小鼠肾脏组织转录组学数据发现,低氧诱导肾脏组织的DEGs主要富集在IL-17、PPAR、mTOR、AMPK、凝血与补体、B细胞受体等炎症反应相关通路。将DEGs与炎症数据库关联筛选出123个IR-DEGs,KEGG和GO富集分析显示,IR-DEGs在细胞因子、炎症反应的调节、炎症应答等通路显著富集。

本研究通过构建PPI网络筛选出STAT3、NFKBIA、CD68、TLR7、LEP和APOE 6个关键基因。CD68是巨噬细胞中表达的跨膜糖蛋白,常作为巨噬细胞的特异性标志物。低氧环境可以通过激活HIF通路,促进CD68等炎症相关基因的表达,导致炎症反应加剧<sup>[17]</sup>。此外,低氧环境还可以诱导巨噬细胞表达CD68等炎症相关标志物,并且通过上调超氧化物歧化酶2的表达,进一步加剧炎症反应<sup>[18]</sup>。低氧环境可以通过多种机制,如激活HIF通路,促进CD68在巨噬细胞中表达等来引发持续的炎症反应。TLR7主要表达于B细胞、树突状细胞中,在免疫调控、炎症作用方面发挥关键作用。TLR7通过MyD88依赖途径发挥作用,募集IL-1受体激酶4,通过NF-κB介导干扰素的产生,促进促炎细胞因子的信号转导<sup>[19]</sup>。研究显示<sup>[20]</sup>,TLR7激动剂可诱导Th1型细胞免疫应答,释放细胞因子,并激活巨噬细胞,提升巨噬细胞的吞噬能力。本研究结果提示,高原低氧环境通过上调TLR7 mRNA与蛋白表达来刺激机体发生炎症反应。研究<sup>[21-22]</sup>表明,低氧上调HIF-1α来增强LEP基因的转录活性,同时上调LEP受体的转录和翻译,从而增加细胞对LEP的响应性。LEP由脂肪细胞分泌,在炎症急性期,LEP促进脂肪细胞分泌炎性细胞因子,同时降低IL-10等抗炎介质的分泌。此外,低氧环境还通过刺激中性粒细胞的趋化活性和ROS的产生来引发炎症反应<sup>[23-24]</sup>。低氧暴露导致LEP水平升高,提示低氧通过上调LEP的表达诱导机体发生炎症反

应。APOE是广泛存在于星形胶质细胞中发挥脂质代谢调控功能的糖蛋白。研究<sup>[25]</sup>表明,在低氧或缺氧条件下,细胞内会产生大量ROS,从而导致APOE的表达和分泌增加,这可能是一种细胞应对氧化应激的适应性机制。APOE与增强炎症反应相关,研究<sup>[26]</sup>发现APOE可以通过调节NF-κB信号级联反应来增强大脑炎症反应,从而导致神经退行性变。低氧暴露使APOE水平升高,表明低氧通过提高APOE水平诱导炎症反应。

STAT3在细胞炎症和免疫调控等方面具有重要作用<sup>[27]</sup>,它由多种细胞因子激活,并作用于细胞表面的多肽发挥生物学效应<sup>[28]</sup>。活化的STAT3促进IL-6与凋亡基因的表达以诱导炎症反应<sup>[29-30]</sup>。已有研究<sup>[31]</sup>证实过度活化的STAT3可以诱导下游TNF-α表达增加。本研究结果显示,低氧暴露下STAT3 mRNA表达显著增高而蛋白表达显著下调,这表明低氧刺激可能使STAT3发生磷酸化或乙酰化而激活来诱导炎症反应。NFKBIA作为NF-κB抑制剂家族成员,在失活状态下与NF-κB/REL复合物形成三聚体存在于胞质中<sup>[32]</sup>。当外界刺激激活通路时,NF-κB抑制蛋白激酶使NFKBIA蛋白发生磷酸化、泛素化并降解,释放NF-κB复合物,经过转位进入细胞核,从而发挥炎性细胞因子转录调控作用,诱发炎症反应<sup>[33]</sup>。本研究发现,低氧刺激使NFKBIA表达上调并抑制NF-κB通路降低炎症刺激,以适应低氧应激损伤。

综上所述,STAT3、CD68、NFKBIA、LEP、TLR7和APOE是低氧诱导炎症反应的关键基因。低氧环境通过上调机体TLR7、CD68、STAT3、LEP、APOE的表达,诱导小鼠肾脏组织发生炎症反应。本研究明确了高原低氧可诱导小鼠肾脏组织发生炎症反应并造成病理损伤,进一步筛选出了低氧诱导小鼠肾脏组织发生炎症反应的关键基因,为高原医学研究提供了新的理论依据。

#### 参考文献:

- [1] BILO G, CARAVITA S, TORLASCO C, et al. Blood pressure at high altitude: physiology and clinical implications [J]. *Kardiol Pol*, 2019, 77(6): 596-603. DOI: 10.33963/KP.14832.
- [2] LI YH, ZHANG YJ, ZHANG Y. Research advances in pathogenesis and prophylactic measures of acute high altitude illness [J]. *Respir Med*, 2018, 145: 145-152. DOI: 10.1016/j.rmed.2018.11.004.
- [3] EVANS RG, SMITH DW, LEE CJ, et al. What makes the kidney susceptible to hypoxia? [J]. *Anat Rec*, 2020, 303(10): 2544-2552. DOI:

- 10.1002/ar.24260.
- [4] ZHOU XM. Reducing oxygen demand to alleviate acute kidney injury [J]. *Front Biosci (Landmark Ed)*, 2023, 28 (3) : 62. DOI: 10.31083/j.fbl2803062.
- [5] PHAM K, PARIKH K, HEINRICH EC. Hypoxia and inflammation: insights from high-altitude physiology [J]. *Front Physiol*, 2021, 12: 676782. DOI: 10.3389/fphys.2021.676782.
- [6] TING KKY, YU P, DOW R, et al. Oxidized low-density lipoprotein accumulation suppresses glycolysis and attenuates the macrophage inflammatory response by diverting transcription from the HIF-1 $\alpha$  to the Nr1 $\beta$  pathway [J]. *J Immunol*, 2023, 211 (10) : 1561-1577. DOI: 10.4049/jimmunol.2300293.
- [7] MERELLI A, REPETTO M, LAZAROWSKI A, et al. Hypoxia, oxidative stress, and inflammation: three faces of neurodegenerative diseases [J]. *J Alzheimers Dis*, 2021, 82 (s1) : S109-S126. DOI: 10.3233/JAD-201074.
- [8] LI L, ZHANG YL, LIU XY, et al. Periodontitis exacerbates and promotes the progression of chronic kidney disease through oral flora, cytokines, and oxidative stress [J]. *Front Microbiol*, 2021, 12: 656372. DOI: 10.3389/fmicb.2021.656372.
- [9] VODOŠEK HOJS N, BEVC S, EKART R, et al. Oxidative stress markers in chronic kidney disease with emphasis on diabetic nephropathy [J]. *Antioxidants*, 2020, 9 (10) : 925. DOI: 10.3390/antiox9100925.
- [10] IRAZABAL MV, TORRES VE. Reactive oxygen species and redox signaling in chronic kidney disease [J]. *Cells*, 2020, 9 (6) : 1342. DOI: 10.3390/cells9061342.
- [11] WU JH, GUO NF, CHEN XL, et al. Coexistence of micro-inflammatory and macrophage phenotype abnormalities in chronic kidney disease [J]. *Int J Clin Exp Pathol*, 2020, 13 (2) : 317-323.
- [12] OLIVIER V, DUNYACH-REMY C, CORBEAU P, et al. Factors of microinflammation in non-diabetic chronic kidney disease: a pilot study [J]. *BMC Nephrol*, 2020, 21 (1) : 141. DOI: 10.1186/s12882-020-01803-y.
- [13] KORBECKI J, SIMIŃSKA D, GAŚSOWSKA-DOBROWOLSKA M, et al. Chronic and cycling hypoxia: drivers of cancer chronic inflammation through HIF-1 and NF- $\kappa$ B activation: a review of the molecular mechanisms [J]. *Int J Mol Sci*, 2021, 22 (19) : 10701. DOI: 10.3390/ijms221910701.
- [14] ZHANG RJ, SAREDY J, SHAO Y, et al. End-stage renal disease is different from chronic kidney disease in upregulating ROS-modulated proinflammatory secretome in PBMCs—a novel multiple-hit model for disease progression [J]. *Redox Biol*, 2020, 34: 101460. DOI: 10.1016/j.redox.2020.101460.
- [15] YU WH, TU YM, LONG Z, et al. Reactive oxygen species bridge the gap between chronic inflammation and tumor development [J]. *Oxid Med Cell Longev*, 2022, 2022: 2606928. DOI: 10.1155/2022/2606928.
- [16] SZKLARCZYK D, GABLE AL, NASTOU KC, et al. The STRING database in 2021: customizable protein-protein networks, and functional characterization of user-uploaded gene/measurement sets [J]. *Nucleic Acids Res*, 2021, 49 (D1) : D605-D612. DOI: 10.1093/nar/gkaa1074.
- [17] WINNING S, FANDREY J. Oxygen sensing in innate immune cells: how inflammation broadens classical hypoxia-inducible factor regulation in myeloid cells [J]. *Antioxid Redox Signal*, 2022, 37 (13-15): 956-971. DOI: 10.1089/ars.2022.0004.
- [18] TWISSELMANN N, PAGEL J, KÜNSTNER A, et al. Hyperoxia/hypoxia exposure primes a sustained pro-inflammatory profile of pre-term infant macrophages upon LPS stimulation [J]. *Front Immunol*, 2021, 12: 762789. DOI: 10.3389/fimmu.2021.762789.
- [19] BENDER AT, TZVETKOV E, PEREIRA A, et al. TLR7 and TLR8 differentially activate the IRF and NF- $\kappa$ B pathways in specific cell types to promote inflammation [J]. *Immuno Horizons*, 2020, 4 (2) : 93-107. DOI: 10.4049/immunohorizons.2000002.
- [20] DE SILVA SENAPATHI U, ABOELKHAIR M, PURO K, et al. In ovo delivered toll-like receptor 7 ligand, resiquimod enhances host responses against infectious bronchitis Corona virus (IBV) infection [J]. *Vaccines*, 2020, 8 (2) : 186. DOI: 10.3390/vaccines8020186.
- [21] KLAFFENBACH D, MEISSNER U, RAAKE M, et al. Upregulation of leptin-receptor in placental cells by hypoxia [J]. *Regul Pept*, 2011, 167 (1) : 156-162. DOI: 10.1016/j.regpep.2010.12.007.
- [22] AMBROSINI G, NATH AK, SIERRA-HONIGMANN MR, et al. Transcriptional activation of the human leptin gene in response to hypoxia. Involvement of hypoxia-inducible factor 1 [J]. *J Biol Chem*, 2002, 277 (37) : 34601-34609. DOI: 10.1074/jbc.M205172200.
- [23] JUTANT EM, TU L, HUMBERT M, et al. The thousand faces of leptin in the lung [J]. *Chest*, 2021, 159 (1) : 239-248. DOI: 10.1016/j.chest.2020.07.075.
- [24] POETSCH MS, STRANO A, GUAN KM. Role of leptin in cardiovascular diseases [J]. *Front Endocrinol*, 2020, 11: 354. DOI: 10.3389/fendo.2020.00354.
- [25] WYNNE ME, OGUNBONA O, LANE AR, et al. APOE expression and secretion are modulated by mitochondrial dysfunction [J]. *eLife*, 2023, 12: e85779. DOI: 10.7554/eLife.85779.
- [26] ARNAUD L, BENECH P, GREETHAM L, et al. APOE4 drives inflammation in human astrocytes via TAGLN3 repression and NF- $\kappa$ B activation [J]. *Cell Rep*, 2022, 40 (7) : 111200. DOI: 10.1016/j.celrep.2022.111200.
- [27] BENDEK MJ, CANEDO-MARROQUÍN G, REALINI O, et al. Periodontitis and gestational diabetes mellitus: a potential inflammatory vicious cycle [J]. *Int J Mol Sci*, 2021, 22 (21) : 11831. DOI: 10.3390/ijms222111831.
- [28] HILLMER EJ, ZHANG HY, LI HS, et al. STAT3 signaling in immunity [J]. *Cytokine Growth Factor Rev*, 2016, 31: 1-15. DOI: 10.1016/j.cytogr.2016.05.001.
- [29] LIU Y, ZHANG J, ZHOU YH, et al. Activation of the IL-6/JAK2/STAT3 pathway induces plasma cell mastitis in mice [J]. *Cytokine*, 2018, 110: 150-158. DOI: 10.1016/j.cyto.2018.05.002.
- [30] EL-SHERBINY M, EL-SAYED RM, HELAL MA, et al. Nifuroxazide mitigates angiogenesis in ehrlich's solid carcinoma: molecular docking, bioinformatic and experimental studies on inhibition of il-6/Jak2/Stat3 signaling [J]. *Molecules*, 2021, 26 (22) : 6858. DOI: 10.3390/molecules26226858.
- [31] LI HN, YANG QQ, WANG WT, et al. Red nucleus IL-33 facilitates the early development of mononeuropathic pain in male rats by inducing TNF- $\alpha$  through activating ERK, p38 MAPK, and JAK2/STAT3 [J]. *J Neuroinflammation*, 2021, 18 (1) : 150. DOI: 10.1186/s12974-021-02198-9.
- [32] BOISSON B, PUEL A, PICARD C, et al. Human I $\kappa$ B $\alpha$  gain of function: a severe and syndromic immunodeficiency [J]. *J Clin Immunol*, 2017, 37 (5) : 397-412. DOI: 10.1007/s10875-017-0400-z.
- [33] YU H, LIN LB, ZHANG ZQ, et al. Targeting NF- $\kappa$ B pathway for the therapy of diseases: mechanism and clinical study [J]. *Signal Transduct Target Ther*, 2020, 5 (1) : 209. DOI: 10.1038/s41392-020-00312-6.